An Improved Cubic Cardinal Spline and Its Fairing

Juncheng Li, Chengzhi Liu, and Lian Yang

Abstract—**The cubic cardinal spline is an important tool for constructing interpolation curves and surfaces. Global shape adjustment of the cubic cardinal spline can be achieved by modifying the value of the free parameter in the spline. Unfortunately, local shape adjustment of the cubic cardinal spline cannot be achieved through the free parameter. An improved cubic cardinal spline is proposed to tackle this issue. The improved cubic cardinal spline retains the characteristics of the traditional cubic cardinal spline and can also make local adjustment to the spline using the free parameters. In addition, the method for constructing the fair improved cubic cardinal spline by minimizing the bending energy is given. Numerical examples show that the improved cubic cardinal spline is more practical than the traditional cubic cardinal spline in data interpolation.**

Index Terms—**Interpolation spline, cubic cardinal spline, free parameter, local adjustment, fairing**

I. Introduction

Data interpolation has always been an important research topic in computer-aided design and related fields. The splines that naturally interpolate the data points have attracted much attention when solving data interpolation problems. Such as the cubic Catmull-Rom spine [1], the cubic cardinal spline [2], the positivity-preserving interpolation spline with local free parameters [3, 4], the polynomial interpolation spline with free parameters [5], the quartic Catmull-Rom spline with local parameters [6], and so on. The cubic cardinal spline not only naturally interpolates the data points but also can achieve shape adjustment through the free parameter(s), which makes it applicable in many engineering fields [7, 8]. However, the shape of the cubic cardinal spline can only achieve global adjustment but not local adjustment by utilizing the free parameter(s), which limits its applications in data interpolation problems. To alleviate the shortcomings of the traditional cubic cardinal spline in shape adjustment, this paper constructs an improved cubic cardinal spline. The improved cubic cardinal spline naturally interpolates the data points and can achieve global and local shape adjustment through the free parameters.

Manuscript received June 8, 2024; revised October 9, 2024.

This work was supported by the Hunan Provincial Natural Science Foundation of China under Grant No. 2024JJ7254, and the National Natural Science Foundation of China under Grant No. 12101225.

Juncheng Li is a professor of College of Mathematics and Finance, Hunan University of Humanities, Science and Technology, Loudi 417000, PR China (corresponding author phone: +86 738 8325585; fax: +86 738 8325585; e-mail: lijuncheng82@126.com).

Chengzhi Liu is an associate professor of College of Mathematics and Finance, Hunan University of Humanities, Science and Technology, Loudi 417000, PR China (e-mail: it-rocket@163.com).

Lian Yang is an associate professor of College of Mathematics and Finance, Hunan University of Humanities, Science and Technology, Loudi 417000, PR China (e-mail: ylianyang@163.com).

After the improved cubic cardinal spline is constructed, a further problem naturally arises: how to determine the values of the free parameters in the improved cubic cardinal spline to ensure that the modified spline meets certain specific requirements? It is known that fairing is an important geometric feature of curves and surfaces, and the construction of fair curves and surfaces has long been a fundamental issue in computer-aided design and related fields. Although there is currently no recognized mathematical method to quantify the fairing of curves and surfaces, constructing fair curves and surfaces by energy minimization has become a common approach. Such as the fair B-spline curve [9], the fair Bézier curve [10], the fair interpolation curve and surface [11], the fair Hermit interpolation [12, 13], the fair mesh [14, 15], and so on. Drawing inspiration from these references, this paper gives the method for constructing the fair improved cubic cardinal spline by using the bending energy minimization.

The rest of this paper is organized as follows. In Section II, the definition and properties of the improved cubic cardinal spline curve are presented. In Section III, the method for constructing the fair improved cubic cardinal spline curve using the bending energy minimization is given. In Section IV, the definition and properties of the improved cubic cardinal spline surface, as well as the method for constructing the fair improved cubic cardinal spline surface using the bending energy minimization are provided. Finally, a brief conclusion is given in Section V.

II. The improved cubic Cardinal spline curve

Given a series of data points $\boldsymbol{p}_i \in \mathbb{R}^k$ ($k = 2,3$; $i = 0,1,\cdots,n$; $n \geq 3$), for $0 \leq t \leq 1$, the traditional cubic cardinal spline curve can be expressed as [2]

$$\boldsymbol{S}_i(t) = b_0(\alpha;t)\boldsymbol{p}_i + b_1(\alpha;t)\boldsymbol{p}_{i+1} + b_2(\alpha;t)\boldsymbol{p}_{i+2} + b_3(\alpha;t)\boldsymbol{p}_{i+3}, \quad (1)$$

where $i = 0,1,\cdots,n-3$,

$$\begin{cases} b_0(\alpha;t) = -\alpha t^3 + 2\alpha t^2 - \alpha t, \\ b_1(\alpha;t) = (2-\alpha)t^3 + (\alpha-3)t^2 + 1, \\ b_2(\alpha;t) = (\alpha-2)t^3 + (3-2\alpha)t^2 + \alpha t, \\ b_3(\alpha;t) = \alpha t^3 - \alpha t^2, \end{cases} \quad (2)$$

are the basis functions, and $\alpha > 0$ is a free parameter.

By verifying from Eqs. (1) and (2), the traditional cubic cardinal spline curve naturally interpolates the data points $\boldsymbol{p}_i$ $(i=1,2,\cdots,n-1)$ and satisfies C^1 continuity. In addition, the shape of the traditional cubic cardinal spline curve can be freely adjusted by altering the value of α when all the data points are fixed. Due to these excellent characteristics, the traditional cubic cardinal spline curve has become an important tool for constructing interpolation curves.

Although the free parameter in the traditional cubic cardinal spline curve can be used to freely adjust the shape of the curve while keeping the data points fixed, this shape adjustment is global. This means that modifying the value of the free parameter will change the shape of the entire curve, and cannot achieve local shape adjustment of the curve. In practical applications, many situations require local shape adjustment of the interpolation curves. To this end, the expression of the traditional cubic cardinal spline curve is slightly reformed to construct a locally adjustable cubic cardinal spline curve.

Definition 1 *Given a series of data points* $\boldsymbol{p}_i \in \mathbb{R}^k$ ($k=2,3$ *;* $i=0,1,\cdots,n$ *;* $n \ge 3$), *for* $0 \le t \le 1$, *the curve*

$$\begin{aligned}\boldsymbol{R}_i(t) = f_{i,0}(\alpha_i;t)\boldsymbol{p}_i + f_{i,1}(\alpha_{i+1};t)\boldsymbol{p}_{i+1} + \\ f_{i,2}(\alpha_i;t)\boldsymbol{p}_{i+2} + f_{i,3}(\alpha_{i+1};t)\boldsymbol{p}_{i+3},\end{aligned} \tag{3}$$

is called the improved cubic cardinal spline curve, where $i=0,1,\cdots,n-3$, *and*

$$\begin{cases} f_{i,0}(\alpha_i;t) = -\alpha_i t^3 + 2\alpha_i t^2 - \alpha_i t, \\ f_{i,1}(\alpha_{i+1};t) = (2-\alpha_{i+1})t^3 + (\alpha_{i+1}-3)t^2 + 1, \\ f_{i,2}(\alpha_i;t) = (\alpha_i - 2)t^3 + (3-2\alpha_i)t^2 + \alpha_i t, \\ f_{i,3}(\alpha_{i+1};t) = \alpha_{i+1}t^3 - \alpha_{i+1}t^2, \end{cases} \tag{4}$$

are the basis functions, $\alpha_i > 0$ $(i=0,1,\cdots,n-2)$ *are the free parameters.*

It is easy to find that the improved cubic cardinal spline curve is the traditional cubic cardinal spline curve when $\alpha_i = \alpha$ $(i=0,1,\cdots,n-2)$.

Theorem 1 *The improved cubic cardinal spline curve has properties as follows,*

(a) Interpolation. The spline curve naturally interpolates the data points $\boldsymbol{p}_i$ $(i=1,2,\cdots,n-1)$.

(b) Continuity. The spline curve satisfies C^1 *continuity.*

(c) Shape adjustability. When the data points $\boldsymbol{p}_i$ $(i=0,1,\cdots,n)$ *are kept unchanged, the shape of the spline curve can be locally and globally adjusted by altering the values of the free parameters* α_i $(i=0,1,\cdots,n-2)$.

Proof (a) It can be calculated from Eqs. (3) and (4) that

$$\boldsymbol{R}_i(0) = \boldsymbol{p}_{i+1}, \ \boldsymbol{R}_i(1) = \boldsymbol{p}_{i+2}, \ i=0,1,\cdots,n-3. \tag{5}$$

Eq. (5) shows that the spline curve naturally interpolates the data points $\boldsymbol{p}_i$ $(i=1,2,\cdots,n-1)$.

(b) By further calculation from Eqs. (3) and (4), it can be concluded that

$$\boldsymbol{R}_i'(0) = \alpha_i(\boldsymbol{p}_{i+2} - \boldsymbol{p}_i), \ \boldsymbol{R}_i'(1) = \alpha_{i+1}(\boldsymbol{p}_{i+3} - \boldsymbol{p}_{i+1}). \tag{6}$$

Eqs. (5) and (6) show that $\boldsymbol{R}_i^{(k)}(1) = \boldsymbol{R}_{i+1}^{(k)}(0)$ $(k=0,1)$, which indicates that the spline curve satisfies C^1 continuity.

(c) From Eqs. (3) and (4), changing the value of α_j $(j \in \{0, n-2\})$ will only affect the shape of $\boldsymbol{R}_j(t)$, changing the value of α_k $(k \in \{1,2,\cdots,n-3\})$ will only affect the shape of $\boldsymbol{R}_{k-1}(t)$ and $\boldsymbol{R}_k(t)$. That means α_i $(i=0,1,\cdots,n-2)$ in the spline curve are local. If $\alpha_i = \alpha$ $(i=0,1,\cdots,n-2)$, the shape of the spline curve can be global adjusted by changing the value of α.

Example 1 Given the data points

$\boldsymbol{p}_0=(35,47)$, $\boldsymbol{p}_1=(16,40)$, $\boldsymbol{p}_2=(15,15)$,
$\boldsymbol{p}_3=(25,36)$, $\boldsymbol{p}_4=(40,15)$, $\boldsymbol{p}_5=(65,25)$,
$\boldsymbol{p}_6=(50,40)$, $\boldsymbol{p}_7=(60,42)$, $\boldsymbol{p}_8=(80,37)$.

When the data points are fixed, the local shape adjustment of the planar improved cubic cardinal spline curve through the free parameters is shown in Fig. 1. In Fig. 1(a), α_0 is taken as 0.2, 0.5, and 0.9, respectively, while all other parameters are taken as 0.5. In Fig. 1(b), α_2 is taken as 0.2, 0.5, and 0.9, respectively, while all other parameters are taken as 0.5.

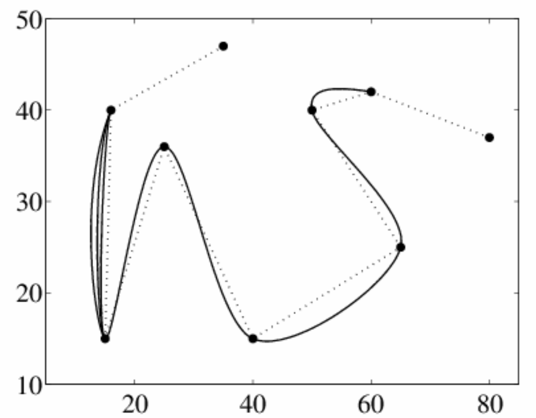

(a) Modifying the value of α_0

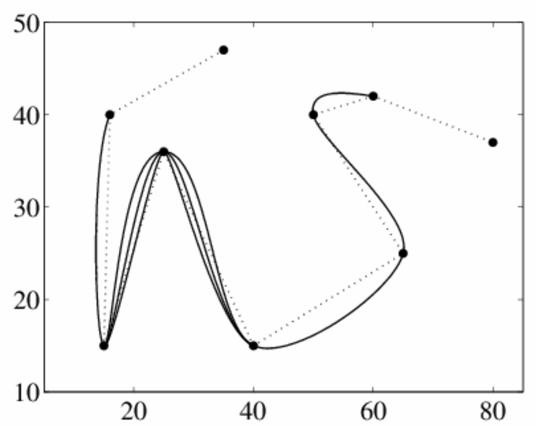

(b) Modifying the value of α_2

Fig. 1 The local shape adjustment of the planar improved cubic cardinal spline curve through the free parameters

When the data points are fixed, the global shape adjustment of the planar improved cubic cardinal spline curve through the free parameter α is shown in Fig. 2.

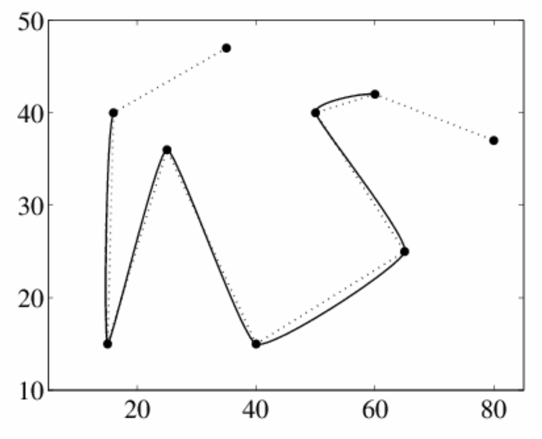

(a) $\alpha = 0.2$

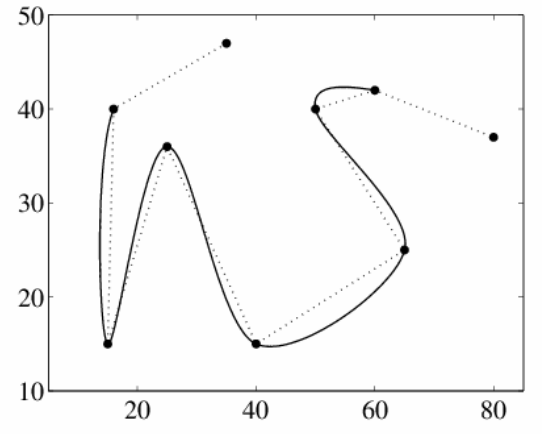

(b) $\alpha = 0.5$

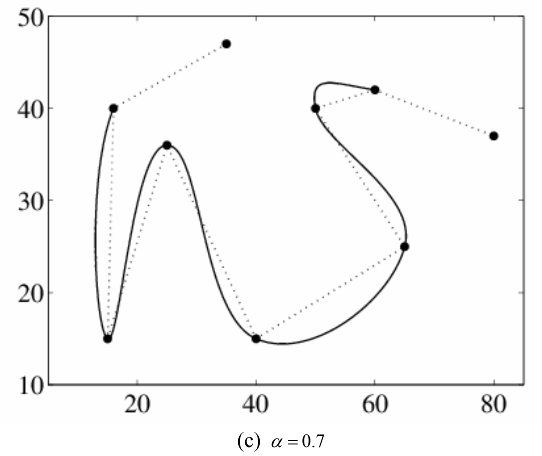

(c) $\alpha = 0.7$

Fig. 2 The global shape adjustment of the planar improved cubic cardinal spline curve through the free parameter

Example 2 Taken the following data points from a cylindrical helix,

$$\boldsymbol{p}_i = \left(\cos(i\pi/2 + (-1)^i \pi/12), \sin(i\pi/2 + (-1)^i \pi/12),\right.$$
$$\left.(i\pi/2 + (-1)^i \pi/12)/5\right),\ i = 0,1,\cdots,10\,.$$

When the data points are fixed, the local shape adjustment of the spatial improved cubic cardinal spline curve through the free parameters is shown in Fig. 3. In Fig. 3(a), α_2 is taken as 0.2, 0.7, and 1.2, respectively, while all other parameters are taken as 0.5. In Fig. 3(b), α_8 is taken as 0.2, 0.7, and 1.2, respectively, while all other parameters are taken as 0.5.

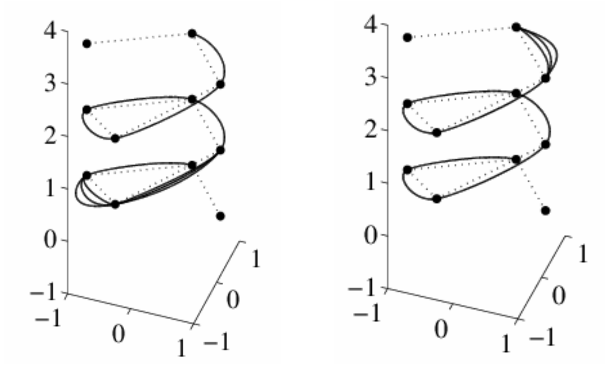

(a) Modifying the value of α_2 (b) Modifying the value of α_8

Fig. 3 The local shape adjustment of the spatial improved cubic cardinal spline curve through the free parameters

When the data points are fixed, the global shape adjustment of the spatial improved cubic cardinal spline curve through the free parameter α is shown in Fig. 4.

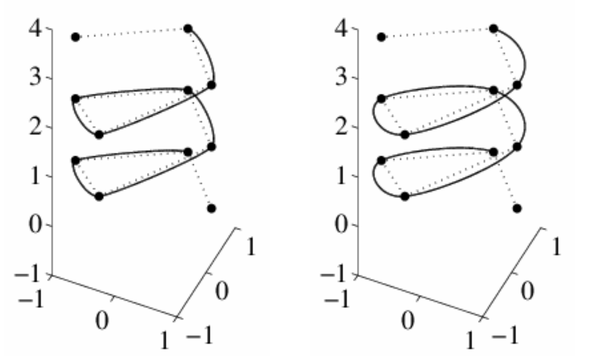

(a) $\alpha = 0.3$ (b) $\alpha = 0.6$

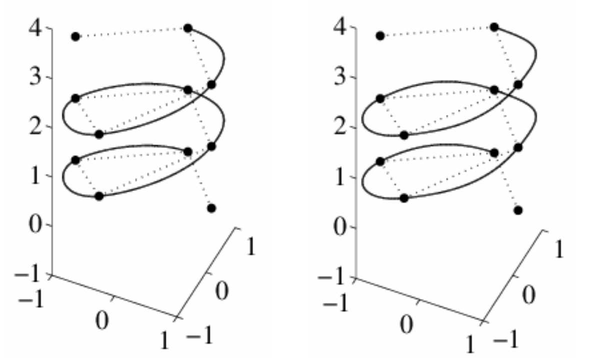

(c) $\alpha = 0.8$ (d) $\alpha = 1.0$

Fig. 4 The global shape adjustment of the spatial improved cubic cardinal spline curve through the free parameter

Remark 1 According to Eq. (6), the tangent length of the improved cubic cardinal spline segment $\boldsymbol{R}_i(t)$ at both ends is determined by the free parameters $\alpha_i\ (i = 0,1,\cdots,n-2)$. If the values of α_i are too small or too large, it may cause the generated curve to exhibit sharp points, self-intersection, and other phenomena. It is necessary to reasonably set the range of α_i in practical applications. Hence, let

$$D_1 = \{\alpha_i \mid 0 < l_i \le \alpha_i \le u_i,\ i = 0,1,\cdots,n-2\}\,,$$

where l_i and u_i are given non-negative numbers. For convenience, it is advisable to set

$$l_i := l\,,\ u_i := u\ \ (i = 0,1,\cdots,n-2)\,,$$

and take the specific values of l and u as needed. This paper suggests taking $l=0.1$, $u=3$, that is,

$$D_1=\{\alpha_i \mid 0.1 \le \alpha_i \le 3,\ i=0,1,\cdots,n-2\}.$$

III. Fairing of the Spline Curve

Due to the free parameters, the improved cubic cardinal spline curve can achieve local and global shape adjustment while keeping the data points fixed, which provides convenience for constructing interpolation curves.

However, people may sometimes need to determine the specific values of the free parameters in the improved cubic cardinal spline curve to obtain the curve as fair as possible. In recent years, using the bending energy (also known as strain energy) minimization to construct fair curves has become a common method [9-13]. For the parametric curve $\boldsymbol{b}(t)$ $(a \le t \le b)$, its bending energy can be approximately expressed as [9, 10],

$$E_1=\int_a^b \left\|\boldsymbol{b}''(t)\right\|^2 \mathrm{d}t. \tag{7}$$

From Eq. (3), the entire improved cubic cardinal spline curve is composed of $n-2$ segments. According to Eq. (7), the bending energy of the entire improved cubic cardinal spline curve can be approximately expressed as

$$E_1=\sum_{i=0}^{n-3}\int_0^1 \left\|\boldsymbol{R}_i''(t)\right\|^2 \mathrm{d}t. \tag{8}$$

From Eq. (4), Eq. (3) can be rewritten as

$$\boldsymbol{R}_i(t)=\boldsymbol{A}_i(t)\alpha_i+\boldsymbol{B}_i(t)\alpha_{i+1}+\boldsymbol{C}_i(t), \tag{9}$$

where

$\boldsymbol{A}_i(t):=t(1-t)^2(\boldsymbol{p}_{i+2}-\boldsymbol{p}_i)$, $\boldsymbol{B}_i(t):=-t^2(1-t)(\boldsymbol{p}_{i+3}-\boldsymbol{p}_{i+1})$,
$\boldsymbol{C}_i(t):=\boldsymbol{p}_{i+1}+t^2(3-2t)(\boldsymbol{p}_{i+2}-\boldsymbol{p}_{i+1})$, $i=0,1,\cdots,n-3$.

By substituting Eq. (9) into Eq. (8), then

$$\begin{aligned}E_1=\sum_{i=0}^{n-3}\Big(&\alpha_i^2\int_0^1\left\|\boldsymbol{A}_i''(t)\right\|^2\mathrm{d}t+\alpha_{i+1}^2\int_0^1\left\|\boldsymbol{B}_i''(t)\right\|^2\mathrm{d}t+\\&2\alpha_i\alpha_{i+1}\int_0^1\left(\boldsymbol{A}_i''(t)\cdot\boldsymbol{B}_i''(t)\right)\mathrm{d}t+2\alpha_i\int_0^1\left(\boldsymbol{A}_i''(t)\cdot\boldsymbol{C}_i''(t)\right)\mathrm{d}t+\\&2\alpha_{i+1}\int_0^1\left(\boldsymbol{B}_i''(t)\cdot\boldsymbol{C}_i''(t)\right)\mathrm{d}t+\int_0^1\left\|\boldsymbol{C}_i''(t)\right\|^2\mathrm{d}t\Big).\end{aligned} \tag{10}$$

It is clear that E_1 in Eq. (10) is a function of α_i $(i=0, 1,\cdots,n-2)$. Then the following optimization model needs to be solved for constructing the fair improved cubic cardinal spline curve,

$$\min_{(\alpha_0,\alpha_1,\cdots,\alpha_{n-2})\in D_1} E_1(\alpha_0,\alpha_1,\cdots,\alpha_{n-2}). \tag{11}$$

From Eq. (10), it can be seen that $E_1(\alpha_0,\alpha_1,\cdots,\alpha_{n-2})$ is a multivariate quadratic polynomial function. It is easy to obtain the solution of Eq. (11) using some mathematical software.

Remark 2 For comparative analysis, the bending energy minimization is also used to construct the fair traditional cubic cardinal spline curve. According to Eq. (2), Eq. (1) can be rewritten as follows,

$$\boldsymbol{S}_i(t)=\boldsymbol{G}_i(t)\alpha+\boldsymbol{H}_i(t), \tag{12}$$

where

$\boldsymbol{G}_i(t):=(t^3-2t^2+t)(\boldsymbol{p}_{i+2}-\boldsymbol{p}_i)+(t^3-t^2)(\boldsymbol{p}_{i+3}-\boldsymbol{p}_{i+1})$,
$\boldsymbol{H}_i(t):=\boldsymbol{p}_{i+1}+(-2t^3+3t^2)(\boldsymbol{p}_{i+2}-\boldsymbol{p}_{i+1})$, $i=0,1,\cdots,n-3$.

By replacing $\boldsymbol{S}_i(t)$ in Eq. (8) with $\boldsymbol{R}_i(t)$ in Eq. (12), then

$$\begin{aligned}E_1(\alpha)=\sum_{i=0}^{n-3}\Big(&\alpha^2\int_0^1\left\|\boldsymbol{G}_i''(t)\right\|^2\mathrm{d}t+2\alpha\int_0^1(\boldsymbol{G}_i''(t)\cdot\boldsymbol{H}_i''(t))\mathrm{d}t+\\&\int_0^1\left\|\boldsymbol{H}_i''(t)\right\|^2\mathrm{d}t\Big).\end{aligned} \tag{13}$$

Then the following optimization model needs to be solved for constructing the fair traditional cubic cardinal spline curve,

$$\min_{\alpha\in D_1} E_1(\alpha), \tag{14}$$

where $D_1=\{\alpha \mid 0.1\le\alpha\le 3\}$.

From Eq. (13), it can be seen that $E_1(\alpha)$ is a univariate quadratic polynomial function. It is not difficult to obtain the solution of Eq. (11).

Example 3 For the planar data points given in Example 1, by solving Eq. (11) and Eq. (14) respectively yields:

(a) The values of the free parameters in the fair improved cubic cardinal spline curve are

$$\alpha_0=0.8751,\ \alpha_1=0.6218,\ \alpha_2=0.4232,$$
$$\alpha_3=0.6770,\ \alpha_4=0.6369,\ \alpha_5=0.6490,\ \alpha_6=0.5569.$$

(b) The values of the free parameter in the fair traditional cubic cardinal spline curve is $\alpha=0.6402$.

The bending energy of the two planar fair cubic cardinal spline curves are shown in Table I.

TABLE I
THE BENDING ENERGY OF THE TWO PLANAR FAIR CURVES

Spline curve	Bending energy
The fair improved cubic cardinal spline curve	1.9124×10^4
The fair traditional cubic cardinal spline curve	1.9691×10^4

Table I shows that the bending energy of the planar fair improved cubic cardinal spline curve is smaller than that of the planar fair traditional cubic cardinal spline curve. The two planar fair cubic cardinal spline curves and their curvature graphs are shown in Fig. 5.

Fig. 5 shows that the curvature variation of the first and second segments of the planar fair improved cubic cardinal spline curve is smaller than that of the planar fair traditional cubic cardinal spline curve, and the curvature variation of other segments of the planar fair improved cubic cardinal spline curve is almost the same as that of the planar fair traditional cubic cardinal spline curve. These indicate that the curvature variation of the planar fair improved cubic cardinal spline curve is better overall than that of the planar fair traditional cubic cardinal spline curve.

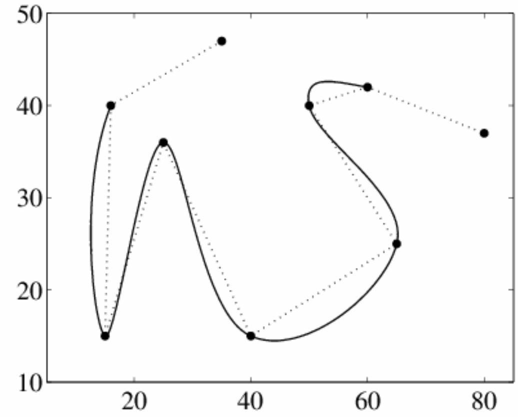

(a) The fair improved spline curve

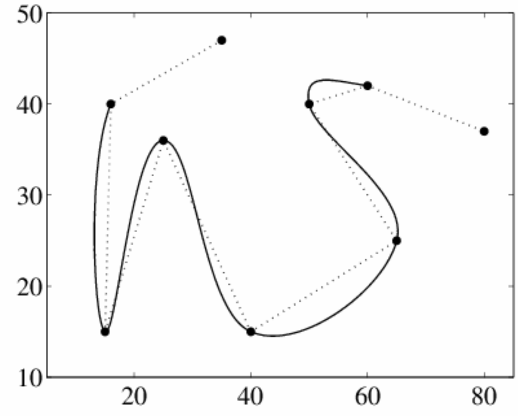

(b) The fair traditional spline curve

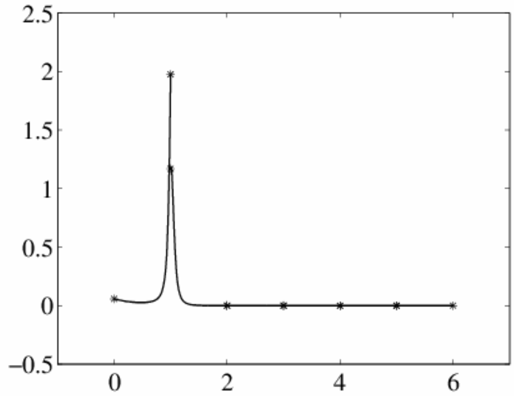

(c) The curvature graph of the fair improved spline curve

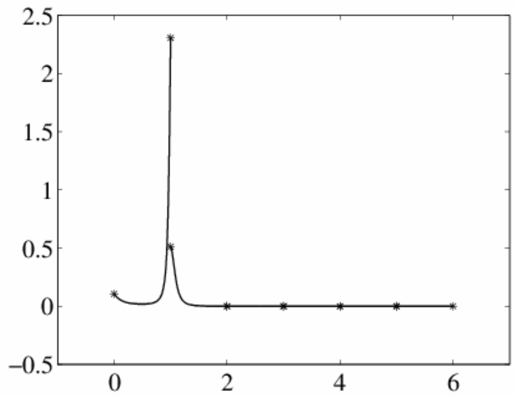

(d) The curvature graph of the fair traditional spline curve

Fig. 5 The two planar fair spline curves and their curvature graphs

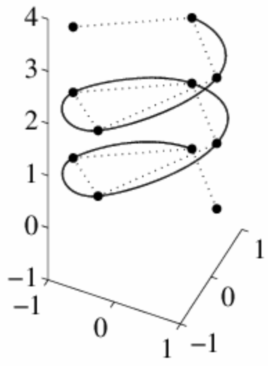

(a) The fair improved spline curve

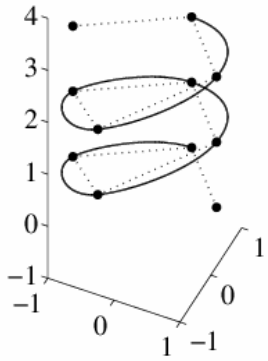

(b) The fair traditional spline curve

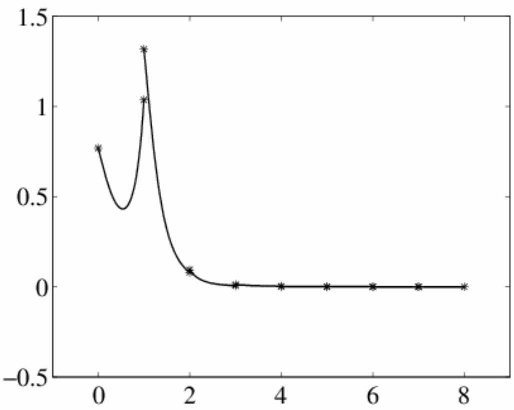

(c) The curvature graph of the fair improved spline curve

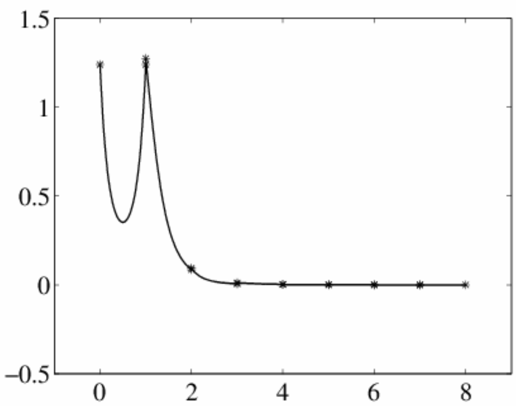

(d) The curvature graph of the fair traditional spline curve

Fig. 6 The two spatial fair spline curves and their curvature graphs

Example 4 For the spatial data points given in Example 2, by solving Eq. (11) and Eq. (14) respectively yields:

(a) The values of the free parameters in the fair improved cubic cardinal spline curve are

$$\alpha_0 = 0.9260\ ,\ \alpha_1 = 0.6891\ ,\ \alpha_2 = 0.7151\ ,$$

$\alpha_3 = 0.7181$, $\alpha_4 = 0.7178$, $\alpha_5 = 0.7180$,
$\alpha_6 = 0.7204$, $\alpha_7 = 0.6988$, $\alpha_8 = 0.5139$.

(b) The values of the free parameter in the fair traditional cubic cardinal spline curve is $\alpha = 0.7178$.

The bending energy of the two spatial fair cubic cardinal spline curves are shown in Table II.

TABLE II
THE BENDING ENERGY OF THE TWO SPATIAL FAIR CURVES

Spline curve	Bending energy
The fair improved cubic cardinal spline curve	49.6637
The fair traditional cubic cardinal spline curve	51.1160

Table II shows that the bending energy of the spatial fair improved cubic cardinal spline curve is also smaller than that of the spatial fair traditional cubic cardinal spline curve. The two spatial fair cubic cardinal spline curves and their curvature graphs are shown in Fig. 6.

Fig. 6 shows that the curvature variation of the first segment of the spatial fair improved cubic cardinal spline curve is smaller than that of the spatial fair traditional cubic cardinal spline curve, and the curvature variation of other segments of the spatial fair improved cubic cardinal spline curve is almost the same as that of the spatial fair traditional cubic cardinal spline curve. These indicate that the curvature variation of the spatial fair improved cubic cardinal spline curve is also better overall than that of the spatial fair traditional cubic cardinal spline curve.

Remark 3. For the convenience of observation, the curvature graphs in Fig. 5 and Fig. 6 are the results of moving the curvature map corresponding to the *i*th segment to the right by *i* units.

IV. THE IMPROVED CUBIC CARDINAL SPLINE SURFACE

A. The Spline Surface

Based on the improved cubic cardinal spline curve, the tensor product spline surface can be defined as follows.

Definition 2. *Given the data points* $\boldsymbol{p}_{i,j}$ ($i = 0,1,\cdots,m$; $j = 0,1,\cdots,n$; $m,n \geq 3$), *for* $0 \leq u,v \leq 1$, *the surface*

$$\boldsymbol{R}_{i,j}(u,v) = \begin{bmatrix} f_{i,0}(\alpha_i;u) & f_{i,1}(\alpha_{i+1};u) & f_{i,2}(\alpha_i;u) & f_{i,3}(\alpha_{i+1};u) \end{bmatrix} \times \begin{bmatrix} \boldsymbol{p}_{i,j} & \boldsymbol{p}_{i,j+1} & \boldsymbol{p}_{i,j+2} & \boldsymbol{p}_{i,j+3} \\ \boldsymbol{p}_{i+1,j} & \boldsymbol{p}_{i+1,j+1} & \boldsymbol{p}_{i+1,j+2} & \boldsymbol{p}_{i+1,j+3} \\ \boldsymbol{p}_{i+2,j} & \boldsymbol{p}_{i+2,j+1} & \boldsymbol{p}_{i+2,j+2} & \boldsymbol{p}_{i+2,j+3} \\ \boldsymbol{p}_{i+3,j} & \boldsymbol{p}_{i+3,j+1} & \boldsymbol{p}_{i+3,j+2} & \boldsymbol{p}_{i+3,j+3} \end{bmatrix} \begin{bmatrix} f_{j,0}(\beta_j;v) \\ f_{j,1}(\beta_{j+1};v) \\ f_{j,2}(\beta_j;v) \\ f_{j,3}(\beta_{j+1};v) \end{bmatrix}, \quad (15)$$

is called the improved cubic cardinal spline surface, where $i = 0,1,\cdots,m-3$; $j = 0,1,\cdots,n-3$; $f_{i,0}(\alpha_i;u)$, $f_{i,1}(\alpha_{i+1};u)$, $f_{i,2}(\alpha_i;u)$, $f_{i,3}(\alpha_{i+1};u)$, $f_{j,0}(\beta_j;v)$, $f_{j,1}(\beta_{j+1};v)$, $f_{j,2}(\beta_j;v)$ *and* $f_{j,3}(\beta_{j+1};v)$ *are the basis functions represented referring to Eq. (4);* $\alpha_i, \beta_j > 0$ ($i = 0,1,\cdots,m-2$; $j = 0,1,\cdots,n-2$) *are the free parameters.*

It is easy to find that the improved cubic cardinal spline surface is the traditional cubic cardinal spline surface when $\alpha_i = \alpha$, $\beta_j = \beta$ ($i = 0,1,\cdots,m-2$; $j = 0,1,\cdots,n-2$).

Theorem 2 *The improved cubic cardinal spline surface has properties as follows,*

(a) Interpolation. The spline surface naturally interpolates the data points $\boldsymbol{p}_{i,j}$ ($i = 1,2,\cdots,m-1$; $j = 1,2,\cdots,n-1$).

(b) Continuity. The spline surface satisfies C^1 *continuity.*

(c) Shape adjustability. When the data points $\boldsymbol{p}_{i,j}$ ($i = 0,1,\cdots,m$; $j = 0,1,\cdots,n$) *are kept unchanged, the shape of the spline surface can be locally and globally adjusted by altering the values of the free parameters* α_i ($i = 1,2,\cdots,m-1$) *and* β_j ($j = 1,2,\cdots,n-1$).

Proof (a) It can be calculated from Eq. (15) that

$$\begin{cases} \boldsymbol{R}_{i,j}(0,0) = \boldsymbol{p}_{i+1,j+1}, & \boldsymbol{R}_{i,j}(0,1) = \boldsymbol{p}_{i+1,j+2}, \\ \boldsymbol{R}_{i,j}(1,0) = \boldsymbol{p}_{i+2,j+1}, & \boldsymbol{R}_{i,j}(1,1) = \boldsymbol{p}_{i+2,j+2}, \end{cases} \quad (16)$$

where $i = 0,1,\cdots,m-3$; $j = 0,1,\cdots,n-3$. Eq. (16) shows that the spline surface naturally interpolates the data points $\boldsymbol{p}_{i,j}$ ($i = 1,2,\cdots,m-1$; $j = 1,2,\cdots,n-1$).

(b) For the convenience of discussion, let

$$f_{i,0} \triangleq f_{i,0}(\alpha_i;u),\ f_{i,1} \triangleq f_{i,1}(\alpha_{i+1};u),$$
$$f_{i,2} \triangleq f_{i,2}(\alpha_i;u),\ f_{i,3} \triangleq f_{i,3}(\alpha_{i+1};u),$$
$$f_{j,0} \triangleq f_{j,0}(\beta_j;v),\ f_{j,1} \triangleq f_{j,1}(\beta_{j+1};v),$$
$$f_{j,2} \triangleq f_{j,2}(\beta_j;v),\ f_{j,3} \triangleq f_{j,3}(\beta_{j+1};v),$$

then it can be calculated from Eq. (15) that

$$\begin{cases} \boldsymbol{R}_{i,j}(0,v) = \sum_{l=0}^{3} f_{j,l}\boldsymbol{p}_{i+1,j+l}, & \boldsymbol{R}_{i,j}(1,v) = \sum_{l=0}^{3} f_{j,l}\boldsymbol{p}_{i+2,j+l}, \\ \boldsymbol{R}_{i,j}(u,0) = \sum_{k=0}^{3} f_{i,k}\boldsymbol{p}_{i+k,j+1}, & \boldsymbol{R}_{i,j}(u,1) = \sum_{k=0}^{3} f_{i,k}\boldsymbol{p}_{i+k,j+2}. \end{cases} \quad (17)$$

$$\begin{cases} \dfrac{\partial \boldsymbol{R}_{i,j}(0,v)}{\partial u} = \alpha_i \sum_{l=0}^{3} f_{j,l}(\boldsymbol{p}_{i+2,j+l} - \boldsymbol{p}_{i,j+l}), \\ \dfrac{\partial \boldsymbol{R}_{i,j}(0,v)}{\partial v} = \sum_{l=0}^{3} f'_{j,l}\boldsymbol{p}_{i+1,j+l}, \\ \dfrac{\partial \boldsymbol{R}_{i,j}(1,v)}{\partial u} = \alpha_{i+1} \sum_{l=0}^{3} f_{j,l}(\boldsymbol{p}_{i+3,j+l} - \boldsymbol{p}_{i+1,j+l}), \\ \dfrac{\partial \boldsymbol{R}_{i,j}(1,v)}{\partial v} = \sum_{l=0}^{3} f'_{j,l}\boldsymbol{p}_{i+2,j+l}. \end{cases} \quad (18)$$

$$\begin{cases} \dfrac{\partial \boldsymbol{R}_{i,j}(u,0)}{\partial u} = \sum_{k=0}^{3} f'_{i,k}\boldsymbol{p}_{i+k,j+1}, \\ \dfrac{\partial \boldsymbol{R}_{i,j}(u,0)}{\partial v} = \beta_j \sum_{k=0}^{3} f_{i,k}(\boldsymbol{p}_{i+k,j+2} - \boldsymbol{p}_{i+k,j}), \\ \dfrac{\partial \boldsymbol{R}_{i,j}(u,1)}{\partial u} = \sum_{k=0}^{3} f'_{i,k}\boldsymbol{p}_{i+k,j+2}, \\ \dfrac{\partial \boldsymbol{R}_{i,j}(u,1)}{\partial v} = \beta_{j+1} \sum_{k=0}^{3} f_{i,k}(\boldsymbol{p}_{i+k,j+3} - \boldsymbol{p}_{i+k,j+1}). \end{cases} \quad (19)$$

From Eqs. (17), (18), and (19), it can be concluded that

$$\begin{cases} \boldsymbol{R}_{i,j}(1,v) = \boldsymbol{R}_{i+1,j}(0,v), \quad \boldsymbol{R}_{i,j}(u,1) = \boldsymbol{R}_{i,j+1}(u,0), \\ \dfrac{\partial \boldsymbol{R}_{i,j}(1,v)}{\partial u} = \dfrac{\partial \boldsymbol{R}_{i+1,j}(0,v)}{\partial u}, \quad \dfrac{\partial \boldsymbol{R}_{i,j}(1,v)}{\partial v} = \dfrac{\partial \boldsymbol{R}_{i+1,j}(0,v)}{\partial v}, \\ \dfrac{\partial \boldsymbol{R}_{i,j}(u,1)}{\partial u} = \dfrac{\partial \boldsymbol{R}_{i,j+1}(u,0)}{\partial u}, \quad \dfrac{\partial \boldsymbol{R}_{i,j}(u,1)}{\partial v} = \dfrac{\partial \boldsymbol{R}_{i,j+1}(u,0)}{\partial v}. \end{cases} \tag{20}$$

Eqs. (16) and (20) show that the spline surface satisfies C^1 continuity.

(c) From Eq. (15), each patch contains the independent free parameters $(\alpha_i, \alpha_{i+1}, \beta_j, \beta_{j+1})$. Thus, changing the values of the free parameters contained in a patch will only have an impact on that patch and its adjacent patches. That means the free parameters α_i $(i = 0,1,\cdots,n-2)$ and β_i $(j = 0,1,\cdots,n-2)$ in the spline surface are local. If $\alpha_i = \alpha$, $\beta_j = \beta$ ($i = 0,1,\cdots,m-2$; $j = 0,1,\cdots,n-2$), the shape of the spline surface can be globally adjusted by changing the value of α and β.

Example 5 Given the data points
$\boldsymbol{p}_{0,0} = (-2,-6,1)$, $\boldsymbol{p}_{0,1} = (-1,-6,1)$, $\boldsymbol{p}_{0,2} = (0,-6,1)$, $\boldsymbol{p}_{0,3} = (1,-6,1)$, $\boldsymbol{p}_{1,0} = (-2,-4,0)$, $\boldsymbol{p}_{1,1} = (-1,-4,0)$, $\boldsymbol{p}_{1,2} = (0,-4,0)$, $\boldsymbol{p}_{1,3} = (1,-4,0)$, $\boldsymbol{p}_{2,0} = (-2,-2,1)$, $\boldsymbol{p}_{2,1} = (-1,-2,1)$, $\boldsymbol{p}_{2,2} = (0,-2,1)$, $\boldsymbol{p}_{2,3} = (1,-2,1)$, $\boldsymbol{p}_{3,0} = (-2,0,1)$, $\boldsymbol{p}_{3,1} = (-1,0,1)$, $\boldsymbol{p}_{3,2} = (0,0,1)$, $\boldsymbol{p}_{3,3} = (1,0,1)$, $\boldsymbol{p}_{4,0} = (-2,2,0)$, $\boldsymbol{p}_{4,1} = (-1,2,0)$, $\boldsymbol{p}_{4,2} = (0,2,0)$, $\boldsymbol{p}_{4,3} = (1,2,0)$, $\boldsymbol{p}_{5,0} = (-2,4,1)$, $\boldsymbol{p}_{5,1} = (-1,4,1)$, $\boldsymbol{p}_{5,2} = (0,4,1)$, $\boldsymbol{p}_{5,3} = (1,4,1)$.

The entire improved cubic cardinal spline surface generated from these data points consists of three patches. The free parameters in the first to third patches are $(\alpha_0, \alpha_1, \beta_0, \beta_1)$, $(\alpha_1, \alpha_2, \beta_0, \beta_1)$, and $(\alpha_2, \alpha_3, \beta_0, \beta_1)$, respectively.

When the data points remain fixed, modifying the value of α_0 or α_3 will have an adjusting effect on the shape of the first or third patch, modifying the values of other free parameters will have an adjusting effect on the shape of at least two patches. Fig. 7 shows the local shape adjustment of the improved cubic cardinal spline surface by modifying the value of the free parameter α_0, with all other free parameters set to 0.5. When the data points are fixed, the global shape adjustment of the improved cubic cardinal spline surface through the free parameters α and β is shown in Fig. 8.

Example 6 Given the data points
$\boldsymbol{p}_{0,0} = (-2,-6,-1)$, $\boldsymbol{p}_{0,1} = (-2,-4,0)$, $\boldsymbol{p}_{0,2} = (-2,-2,-1)$, $\boldsymbol{p}_{0,3} = (-2,0,-1)$, $\boldsymbol{p}_{0,4} = (-2,2,0)$, $\boldsymbol{p}_{0,5} = (-2,4,-1)$, $\boldsymbol{p}_{1,0} = (-1,-6,-1)$, $\boldsymbol{p}_{1,1} = (-1,-4,0)$, $\boldsymbol{p}_{1,2} = (-1,-2,-1)$, $\boldsymbol{p}_{1,3} = (-1,0,-1)$, $\boldsymbol{p}_{1,4} = (-1,2,0)$, $\boldsymbol{p}_{1,5} = (-1,4,-1)$, $\boldsymbol{p}_{2,0} = (0,-6,-1)$, $\boldsymbol{p}_{2,1} = (0,-4,0)$, $\boldsymbol{p}_{2,2} = (0,-2,-1)$, $\boldsymbol{p}_{2,3} = (0,0,-1)$, $\boldsymbol{p}_{2,4} = (0,2,0)$, $\boldsymbol{p}_{2,5} = (0,4,-1)$, $\boldsymbol{p}_{3,0} = (1,-6,-1)$, $\boldsymbol{p}_{3,1} = (1,-4,0)$, $\boldsymbol{p}_{3,2} = (1,-2,-1)$, $\boldsymbol{p}_{3,3} = (1,0,-1)$, $\boldsymbol{p}_{3,4} = (1,2,0)$, $\boldsymbol{p}_{3,5} = (1,4,-1)$.

The entire improved cubic cardinal spline surface generated from these data points consists of three patches. The free parameters in the first to third patches are $(\alpha_0, \alpha_1, \beta_0, \beta_1)$, $(\alpha_0, \alpha_1, \beta_1, \beta_2)$, and $(\alpha_0, \alpha_1, \beta_2, \beta_3)$, respectively.

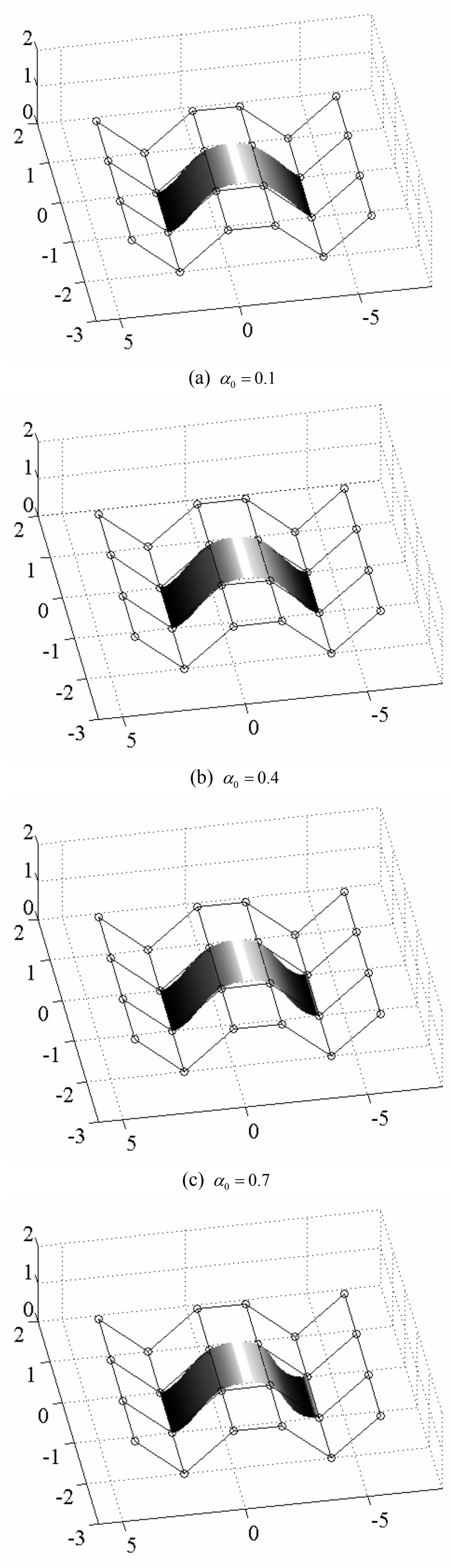

(a) $\alpha_0 = 0.1$

(b) $\alpha_0 = 0.4$

(c) $\alpha_0 = 0.7$

(d) $\alpha_0 = 1.0$

Fig. 7 The local shape adjustment of the improved cubic cardinal spline surface through the free parameter in Example 5

When the data points remain fixed, modifying the value of β_0 or β_3 will have an adjusting effect on the shape of the first or third patch, modifying the values of other free parameters will have an adjusting effect on the shape of at least two patches. Fig. 9 shows the local shape adjustment of the improved cubic cardinal spline surface by modifying the value of free parameter β_3, with all other free parameters set to 0.5.

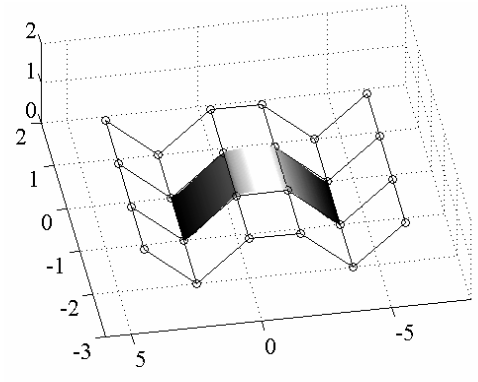

(a) $(\alpha,\beta)=(0.2,0.2)$

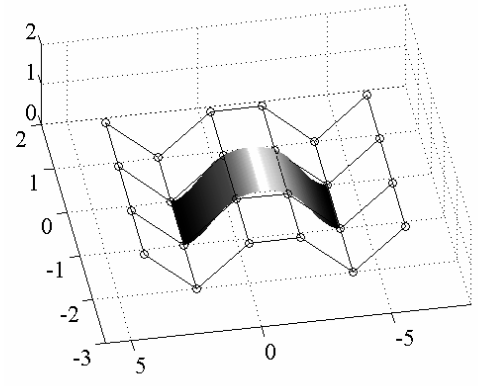

(b) $(\alpha,\beta)=(0.5,0.9)$

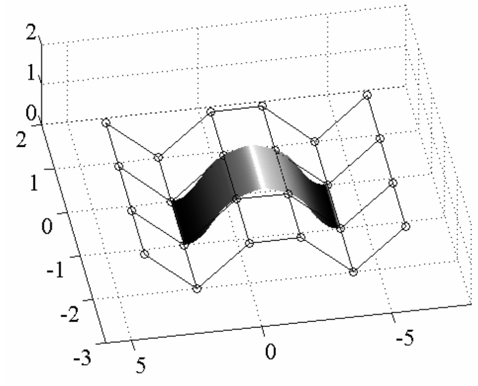

(c) $(\alpha,\beta)=(0.7,1.0)$

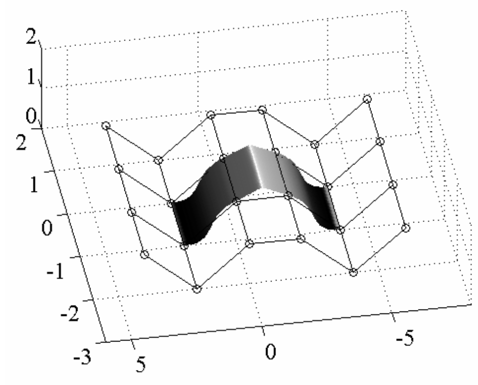

(d) $(\alpha,\beta)=(1.0,1.0)$

Fig. 8 The global shape adjustment of the improved cubic cardinal spline surface through the free parameters in Example 5

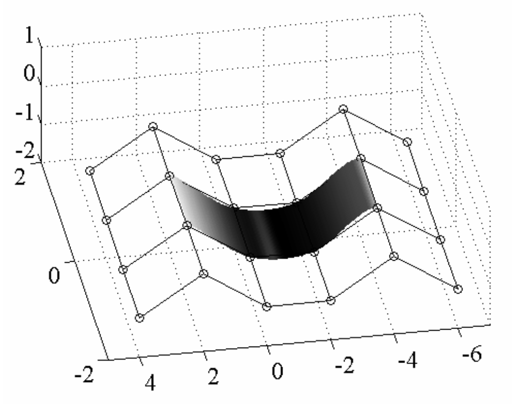

(a) $\beta_3=0.2$

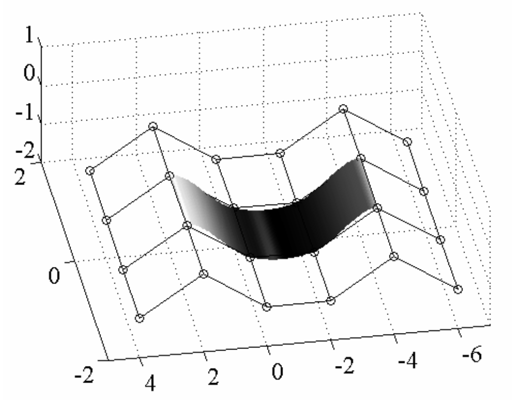

(b) $\beta_3=0.5$

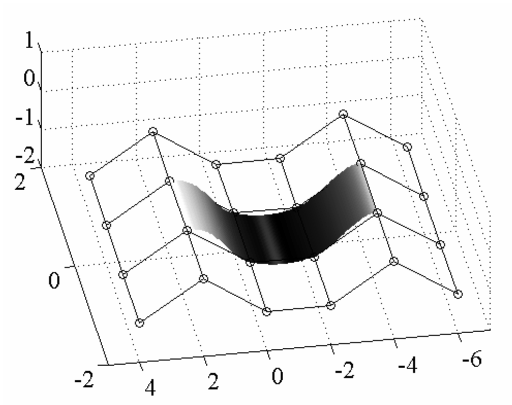

(c) $\beta_3=0.8$

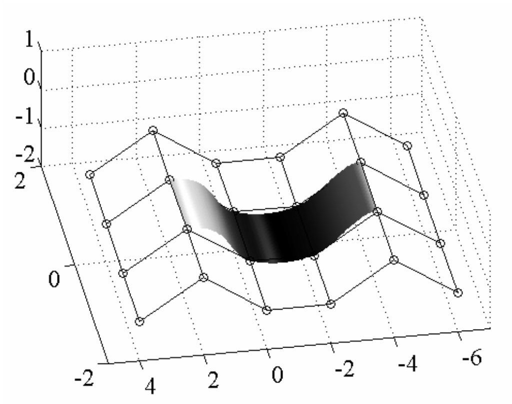

(d) $\beta_3=1.1$

Fig. 9 The local shape adjustment of the improved cubic cardinal spline surface through the free parameter in Example 6

When the data points are fixed, the global shape adjustment of the improved cubic cardinal spline surface through the free parameters α and β is shown in Fig. 10.

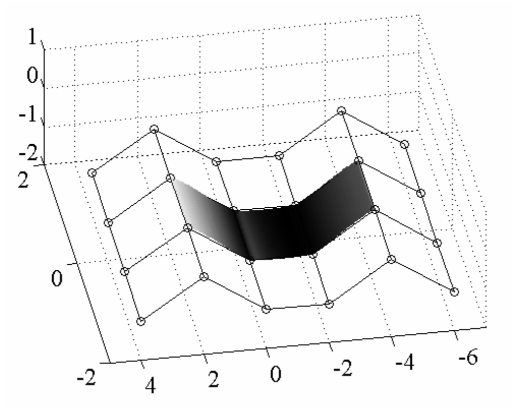

(a) $(\alpha,\beta)=(0.2,0.2)$

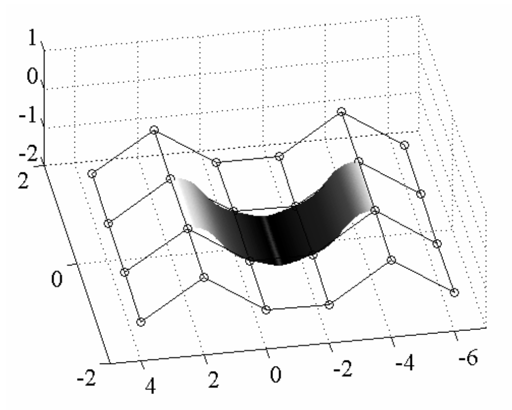

(b) $(\alpha,\beta)=(0.2,0.8)$

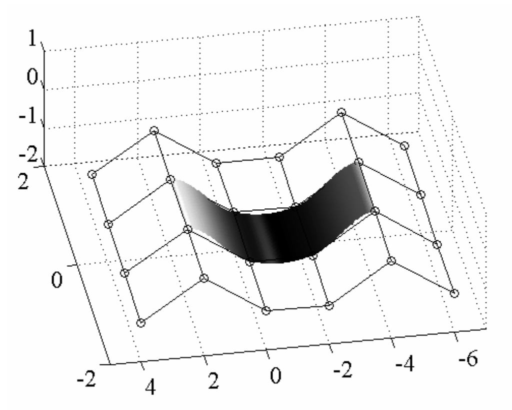

(c) $(\alpha,\beta)=(0.8,0.5)$

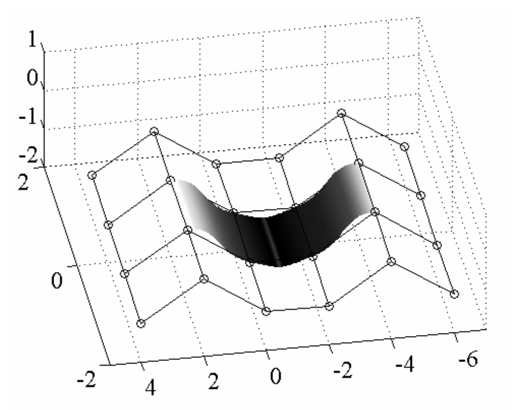

(d) $(\alpha,\beta)=(0.8,0.8)$

Fig. 10 The global shape adjustment of the improved cubic cardinal spline surface through the free parameters in Example 6

Remark 4 Similar to the improved cubic cardinal spline curve, to avoid singularities, self-intersections, and other phenomena in the generated surface, the range of free parameters in the improved cubic cardinal spline surface is set to

$$D_2=\left\{(\alpha_i,\beta_j)\middle|\,0.1\le\alpha_i,\beta_j\le 3,\ i=0,1,\cdots,m-2;\ j=0,1,\cdots,n-2\right\}.$$

B. Fairing of the Spline Surface

Because the second-order generalized thin-plate surface energy (also known as bending energy) can be used to evaluate the fairness of surfaces, it has become a commonly used objective functional for constructing fair surfaces [16]. For the parametric surface $\boldsymbol{s}(u,v)$ $\big((u,v)\in U\big)$, its bending energy can be approximately expressed as [16]

$$E_2=\int_U\left(\|\boldsymbol{s}_{uu}\|^2+2\|\boldsymbol{s}_{uv}\|^2+\|\boldsymbol{s}_{vv}\|^2\right)\mathrm{d}u\mathrm{d}v\,. \tag{21}$$

From Eq. (15), the entire improved cubic cardinal spline surface is composed of $(m-3)\times(n-3)$ patches. According to Eq. (21), the bending energy of the entire improved cubic cardinal spline surface can be approximately expressed as

$$E_2=\sum_{i=0}^{m-3}\sum_{j=0}^{n-3}\int_0^1\int_0^1\left(\left\|\frac{\partial^2\boldsymbol{R}_{i,j}(u,v)}{\partial u^2}\right\|^2+2\left\|\frac{\partial^2\boldsymbol{R}_{i,j}(u,v)}{\partial u\partial v}\right\|^2+\right.$$
$$\left.\left\|\frac{\partial^2\boldsymbol{R}_{i,j}(u,v)}{\partial v^2}\right\|^2\right)\mathrm{d}u\mathrm{d}v\,. \tag{22}$$

Let

$\boldsymbol{A}_{i,j}(u,v):=u(1-u)^2v(1-v)^2(\boldsymbol{p}_{i,j}-\boldsymbol{p}_{i+2,j}+\boldsymbol{p}_{i+2,j+2}-\boldsymbol{p}_{i,j+2})$,

$\boldsymbol{B}_{i,j}(u,v):=u(1-u)^2v^2(1-v)(\boldsymbol{p}_{i+2,j+1}-\boldsymbol{p}_{i,j+1}+\boldsymbol{p}_{i,j+3}-\boldsymbol{p}_{i+2,j+3})$,

$\boldsymbol{C}_{i,j}(u,v):=u^2(1-u)v(1-v)^2(\boldsymbol{p}_{i+3,j}-\boldsymbol{p}_{i+1,j}+\boldsymbol{p}_{i+1,j+2}-\boldsymbol{p}_{i+3,j+2})$,

$\boldsymbol{D}_{i,j}(u,v):=u(1-u)^2v^2(1-v)(\boldsymbol{p}_{i+1,j+1}-\boldsymbol{p}_{i+3,j+1}+\boldsymbol{p}_{i+3,j+3}-\boldsymbol{p}_{i+1,j+3})$,

$\boldsymbol{E}_{i,j}(u,v):=u(1-u)^2(\boldsymbol{p}_{i+2,j+1}-\boldsymbol{p}_{i,j+1})+$
$\quad u(1-u)^2v^2(3-2v)(\boldsymbol{p}_{i,j+1}-\boldsymbol{p}_{i+2,j+1}+\boldsymbol{p}_{i+2,j+2}-\boldsymbol{p}_{i,j+2})$,

$\boldsymbol{F}_{i,j}(u,v):=u^2(1-u)(\boldsymbol{p}_{i+1,j+1}-\boldsymbol{p}_{i+3,j+1})+$
$\quad u^2(1-u)v^2(3-2v)(\boldsymbol{p}_{i+3,j+1}-\boldsymbol{p}_{i+1,j+1}+\boldsymbol{p}_{i+1,j+2}-\boldsymbol{p}_{i+3,j+2})$,

$\boldsymbol{G}_{i,j}(u,v):=v(1-v)^2(\boldsymbol{p}_{i+1,j+2}-\boldsymbol{p}_{i+1,j})+$
$\quad u^2(3-2u)v(1-v)^2(\boldsymbol{p}_{i+1,j}-\boldsymbol{p}_{i+2,j}+\boldsymbol{p}_{i+2,j+2}-\boldsymbol{p}_{i+1,j+2})$,

$\boldsymbol{H}_{i,j}(u,v):=v(1-v)^2(\boldsymbol{p}_{i+1,j+1}-\boldsymbol{p}_{i+1,j+3})+$
$\quad u^2(3-2u)v(1-v)^2(\boldsymbol{p}_{i+2,j+1}-\boldsymbol{p}_{i+1,j+1}+\boldsymbol{p}_{i+1,j+3}-\boldsymbol{p}_{i+2,j+3})$,

$\boldsymbol{I}_{i,j}(u,v):=\boldsymbol{p}_{i+1,j+1}+u^2(3-2u)(\boldsymbol{p}_{i+2,j+1}-\boldsymbol{p}_{i+1,j+1})+$
$\quad v^2(3-2v)(\boldsymbol{p}_{i+1,j+2}-\boldsymbol{p}_{i+1,j+1})+$
$\quad u^2(3-2u)v^2(3-2v)(\boldsymbol{p}_{i+1,j+1}-\boldsymbol{p}_{i+2,j+1}+\boldsymbol{p}_{i+2,j+2}-\boldsymbol{p}_{i+1,j+2})$.

Then Eq. (15) can be rewritten as

$$\begin{aligned}\boldsymbol{R}_{i,j}(u,v)=\;&\boldsymbol{A}_{i,j}(u,v)\alpha_i\beta_j+\boldsymbol{B}_{i,j}(u,v)\alpha_i\beta_{j+1}+\\&\boldsymbol{C}_{i,j}(u,v)\alpha_{i+1}\beta_j+\boldsymbol{D}_{i,j}(u,v)\alpha_{i+1}\beta_{j+1}+\\&\boldsymbol{E}_{i,j}(u,v)\alpha_i+\boldsymbol{F}_{i,j}(u,v)\alpha_{i+1}+\boldsymbol{G}_{i,j}(u,v)\beta_j+\\&\boldsymbol{H}_{i,j}(u,v)\beta_{j+1}+\boldsymbol{I}_{i,j}(u,v),\end{aligned} \tag{23}$$

where $i=0,1,\cdots,m-3$; $j=0,1,\cdots,n-3$.

It is clear that E_2 in Eq. (22) is a function of α_i ($i=0$,

$1,\cdots,m-2)$ and β_j $(j=0,1,\cdots,n-2)$. Then the following optimization model needs to be solved for constructing the fair improved cubic cardinal spline surface,

$$\min_{(\alpha_i,\beta_j)\in D_2} E_2(\alpha_i,\beta_j)\,, \tag{24}$$

where $i=0,1,\cdots,m-2$; $j=0,1,\cdots,n-2$.

From Eqs. (22) and (23), it can be seen that $E_2(\alpha_i,\beta_j)$ is a multivariate quartic polynomial function. It is easy to obtain the solution of Eq. (24) using some mathematical software.

Remark 5 For comparative analysis, the bending energy minimization is also used to construct the fair traditional cubic cardinal spline surface. Let $\alpha_i=\alpha$, $\beta_j=\beta$ ($i=0,1,\cdots,$ $m-2$; $j=0,1,\cdots,n-2$) in Eq. (15), then the traditional cubic cardinal spline surface can be gotten and rewritten as follows,

$$\boldsymbol{R}_{i,j}(u,v)=\boldsymbol{L}_{i,j}(u,v)\alpha\beta+\boldsymbol{M}_{i,j}(u,v)\alpha+\boldsymbol{N}_{i,j}(u,v)\beta+\boldsymbol{I}_{i,j}(u,v)\,, \tag{25}$$

where

$\boldsymbol{L}_{i,j}(u,v):=\boldsymbol{A}_{i,j}(u,v)+\boldsymbol{B}_{i,j}(u,v)+\boldsymbol{C}_{i,j}(u,v)+\boldsymbol{D}_{i,j}(u,v)$,

$\boldsymbol{M}_{i,j}(u,v):=\boldsymbol{E}_{i,j}(u,v)+\boldsymbol{F}_{i,j}(u,v)$,

$\boldsymbol{N}_{i,j}(u,v):=\boldsymbol{G}_{i,j}(u,v)+\boldsymbol{H}_{i,j}(u,v)$,

$i=0,1,\cdots,m-3$; $j=0,1,\cdots,n-3$.

By substituting Eq. (25) into Eq. (22) reveals that the bending energy of the traditional cubic cardinal spline surfaces is a function of α and β. Then the following optimization model needs to be solved for constructing the fair traditional cubic cardinal spline surface,

$$\min_{(\alpha,\beta)\in D_2} E_2(\alpha,\beta)\,, \tag{26}$$

where $D_2=\{(\alpha,\beta)\,|\,0.1\le\alpha,\beta\le 3\}$.

From Eqs. (22) and (25), it can be seen that $E_2(\alpha,\beta)$ is a bivariate quartic polynomial function. It is easy to obtain the solution of Eq. (26) using some mathematical software.

Example 7 For the data points given in Example 5, by solving Eq. (24) and Eq. (26) respectively yields:

(a) The values of the free parameters in the fair improved cubic cardinal spline surface are

$$\alpha_0=0.4900\,,\ \alpha_1=0.5200\,,\ \alpha_2=0.5200\,,$$
$$\alpha_3=0.4900\,,\ \beta_0=1.3405\,,\ \beta_1=0.5905\,.$$

(b) The values of the free parameters in the fair traditional cubic cardinal spline surface are

$$\alpha=0.5102\,,\ \beta=0.5000\,.$$

For the data points given in Example 6, by solving Eq. (24) and Eq. (26) respectively yields:

(a) The values of the free parameters in the fair improved cubic cardinal spline surface are

$$\alpha_0=0.5000\,,\ \alpha_1=0.5000\,,\ \beta_0=1.7926\,,$$
$$\beta_1=1.0426\,,\ \beta_2=0.5512\,,\ \beta_3=\ 0.1000\,.$$

(b) The values of the free parameters in the fair traditional cubic cardinal spline surface are

$$\alpha=0.5000\,,\ \beta=0.1000\,.$$

The two fair cubic cardinal spline surfaces generated from the data points in Example 5 and Example 6 are shown in Fig. 11 and Fig. 12, respectively.

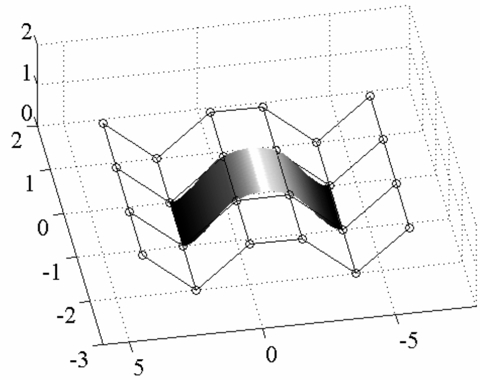

(a) The fair improved surface

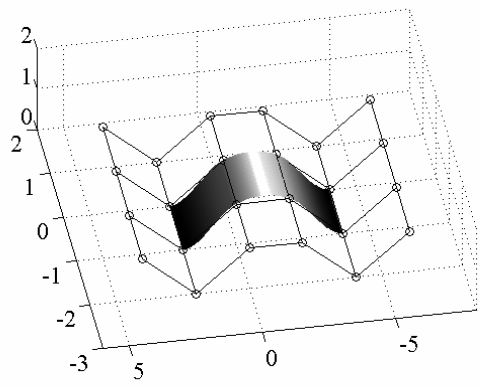

(b) The fair traditional surface

Fig. 11 The two fair surfaces generated from the data points in Example 5

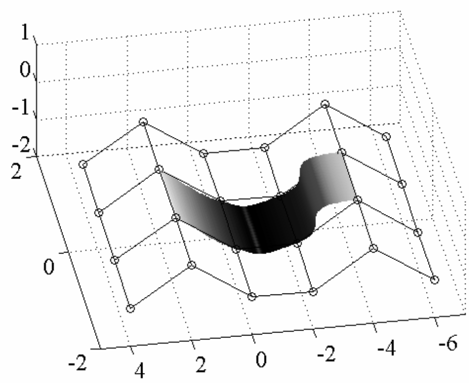

(a) The fair improved surface

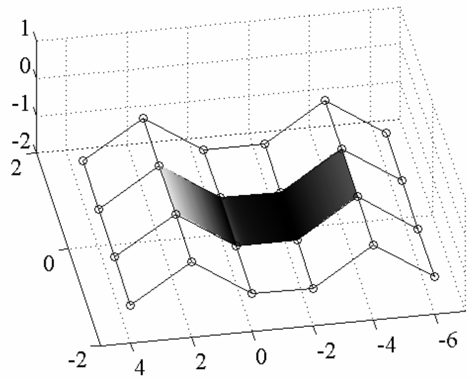

(b) The fair traditional surface

Fig. 12 The two fair surfaces generated from the data points in Example 6

The bending energy of the two fair cubic cardinal spline surfaces generated from the data points in Example 5 and Example 6 is shown in Table III.

TABLE III
THE BENDING ENERGY OF THE TWO FAIR SURFACES

Data points source	Spline surface	Bending energy
Example 5	The fair improved cubic cardinal spline surface	23.8800
	The fair traditional cubic cardinal spline surface	50.9388
Example 6	The fair improved cubic cardinal spline surface	91.6149
	The fair traditional cubic cardinal spline surface	168.2400

Table III shows that the bending energy of the fair improved cubic cardinal spline surface is smaller than that of the fair traditional cubic cardinal spline surface, which indicates that the fairness of the improved cubic cardinal spline surface is generally better than that of the traditional cubic cardinal spline surface.

V. CONCLUSION

An improved cubic cardinal spline is proposed in this paper. The improved spline not only has global adjustability but also local adjustability, which is beneficial for constructing interpolation curves and surfaces. To construct the fair improved cubic cardinal spline, the method for determining the values of the free parameters in the spline using the bending energy minimization is presented. Compared with the fair traditional cubic cardinal spline, the fair improved cubic cardinal spline has better performance.

REFERENCES

[1] T. D. Derose and B. A. Barsky, “Geometric continuity, shape parameters, and geometric constructions for Catmull-Rom splines”, *ACM Transactions on Graphics*, vol. 7, no. 1, pp. 1-41, 1988.

[2] D. Fussel, *Interpolating curves*, University of Texas at Austin, Texas, 2002.

[3] X. B. Qin and Q. S. Xu, “C^1 positivity-preserving interpolation schemes with local free parameters”, *IAENG International Journal of Computer Science*, vol. 43, no. 2, pp. 219-227, 2016.

[4] X. B. Qin and Q. S. Xu, “C^1 rational cubic/linear trigonometric interpolation spline with positivity-preserving property”, *Engineering Letters*, vol. 25, no. 2, pp. 152-159, 2017.

[5] J. C. Li and C. Z. Liu, “A class of polynomial spline curve with free parameters that naturally interpolates the data points”, *IAENG International Journal of Applied Mathematics*, vol. 50, no. 3, pp. 643-647, 2020.

[6] J. C. Li, C. Z. Liu, and G. Ding, “Quartic Catmull-Rom spline function with local parameters and its optimal interpolation”, *Engineering Letters*, vol. 31, no. 3, pp. 1030-1035, 2023.

[7] H. Yoon and T. Park, “Smooth path planning method for autonomous mobile robots using cardinal spline”, *Transactions of the Korean Institute of Electrical Engineers*, vol. 59, no. 4, pp. 803-808, 2010.

[8] A. Fanani, A. Yuniarti, and N. Suciati, “Geometric feature extraction of batik image using Cardinal spline curve representation”, *Telkomnika*, vol. 12, no. 2, pp. 397-404, 2014.

[9] G. Xu, Y. F. Zhu, L. S. Deng, G. Z. Wang, B. J. Li, and K. C. Hui, “Efficient construction of B-spline curves with minimal internal energy”, *Computers, Materials & Continua*, vol. 58, no. 3, pp. 879-892, 2019.

[10] G. Xu, G. Z. Wang, and W. Y. Chen, “Geometric construction of energy-minimizing Bézier curves”, *Science China: Information Sciences*, vol. 54, no. 7, pp. 1395-1406, 2011.

[11] C. M. Zhang, P. F. Zhang, and F. H. Cheng, “Fairing spline curves and surfaces by minimizing energy”, *Computer-Aided Design*, vol. 33, no. 13, pp. 913-923, 2001.

[12] G. Jaklič and E. Žagar, “Planar cubic G^1 interpolatory splines with small strain energy”, *Journal of Computational and Applied Mathematics*, vol. 235, no. 8, pp. 2758–2765, 2011.

[13] L. Z. Lu, “Planar quintic G^2 Hermite interpolation with minimum strain energy”, *Journal of Computational and Applied Mathematics*, vol. 274, pp. 109–117, 2015.

[14] K. Bock and J. Stiller, “Energy-minimizing curve fitting for high-order surfaces mesh generation”, *Applied Mathematics*, vol. 5, pp. 3318-3327, 2014.

[15] K. Bock and J. Stiller, “Optimizing triangular high-order surface meshes by energy-minimization”, *Engineering with Computers*, vol. 34, no. 4, pp. 659-670, 2018.

[16] G. Hu, H. X. Cao, and X. Q. Qin, “Construction of transition surfaces with minimal generalized thin-plate spline-surface energies”, *Computational and Applied Mathematics*, vol. 4, no. 317, 2022.